Electronic Supplementary Material (ESI) for Journal of Materials Chemistry A.

Supplemental information for "Fabrication of FTO-$BiVO_4$-W-WO_3 photoanode for improving photoelectrochemical performance: based on the Z-scheme electron transfer mechanism"

Ruiling Wang[a], Tian Xie[a], Tong Zhang[a], Taofei Pu[a], Yuyu Bu[b*], Jin-Ping Ao[a,b*]

[a]Institute of Technology and Science, Tokushima University, 2-1 Minami-Josanjima, Tokushima 770-8506, Japan.

[b]Key Laboratory of Wide Band-Gap Semiconductor Materials and Devices, School of Microelectronics, Xidian University, Xi'an, 710071, China.

Experimental section

Preparation of $BiVO_4$-W-WO_3 photoanodes

All reagents used in this study were purchased from Sigma-Aldrich Corporation with analytical grade. The purity of gases (Ar, O_2, $SiCl_4$) used in this experiment are higher than 99.999%. The photoanodes were fabricated as we just designed. Firstly, a layer of $BiVO_4$ is deposited on the surface of FTO by the electrochemically deposition method as previous reported [1]. Then W layer which was incompletely oxidized in Ar and O_2 mixed ambient environment (Ar:O_2 = 15:50) was covered on the surface of $BiVO_4$ by magnetron sputtering. We adjusted sputtering time as 800, 1600, 2400, 3200, 4000, 4800 s with a power of 75 W to get the thickness of 50, 100, 150, 200, 250, 300 nm, respectively. Before reactive sputtering, the W target was cleaned by sputtering in an Ar ambient environment for 5 min with a power of 150 W. After rapid thermal annealing (RTA) process at 500℃, WO_3 layer is generated through in-situ oxidation of W layer. The RTA time are 30, 60, 120 min respectively to optimize the PEC performance of the system.

Characterization

The crystalline structures of the thin-films were identified through X-ray diffraction (XRD) (D/MAX-2500/PC; Rigaku Co., Tokyo, Japan). The morphologies of the prepared WO_3 nanoflower structured thin-film photoelectrodes were investigated using scanning electron microscope (SEM) (F250, FEI Company, USA), field emission high-resolution transmission electron microscope (FE-HRTEM, Tecnai G2 F20, FEI Company, USA), and atomic force microscope (AFM, Dimension V, Veeco Instruments Inc. USA). The light absorption properties were investigated using a UV/Vis diffuse reflectance spectrophotometer (UV/Vis DRS, U-41000; HITACHI, Tokyo, Japan). The surface bonding information of the prepared photoanodes were analyzed using X-ray photoelectron spectroscopy (XPS, ULVAC-PHI 5000, Ulvac-Phi, Japan) equipped with a spherical capacitor analyzer and monochromatic Al Kα radiation source (hν = 1486.6 eV) by different etching time.

Photoelectrochemical performance measurements

A three-electrode system was used to test the photoelectrochemical performance of these photoanodes. The photoanode served as the working electrode, a platinum electrode acted as the counter electrode and Ag/AgCl (saturated KCl) served as the reference electrode. The visible light (> 420 nm) with the intensity of 100 $mW \cdot cm^{-2}$ was produced by a 300-W Xe lamp (PLS-SXE 300C, Beijing Perfect light) with a visible light filter. The illumination direction was always front illumination. The photoinduced linear sweep voltammetry I-V curves were measured from -0.2 V to 1.5 V (vs. Ag/AgCl) with a scan rate of 0.05 $V \cdot s^{-1}$. The incident photon-to-current conversion efficiency (IPCE) of the prepared photoanodes were tested at the bias potential of 1.23 V (vs. Ag/AgCl) by a 300-W Xe lamp with a monochromator. The photocurrent stability of $BiVO_4$ and $BiVO_4$-W-WO_3 photoanodes was carried out under a 100 $mW \cdot cm^{-2}$ visible light and 0.5 V (vs. Ag/AgCl) bias potential. All tests were carried out in 0.1 M Na_2SO_4 electrolyte (pH = 7) using the CHI660D electrochemical workstation (Shanghai Chenhua Instrument Co., Ltd., Shanghai, China). The electrochemical impedance spectroscopy (EIS) was also carried out at a bias potential of 0 V under dark and 1.5 V under 100 mW/cm^2

visible light illumination, respectively. The frequency range was from 10^5 to 10^{-1} Hz.

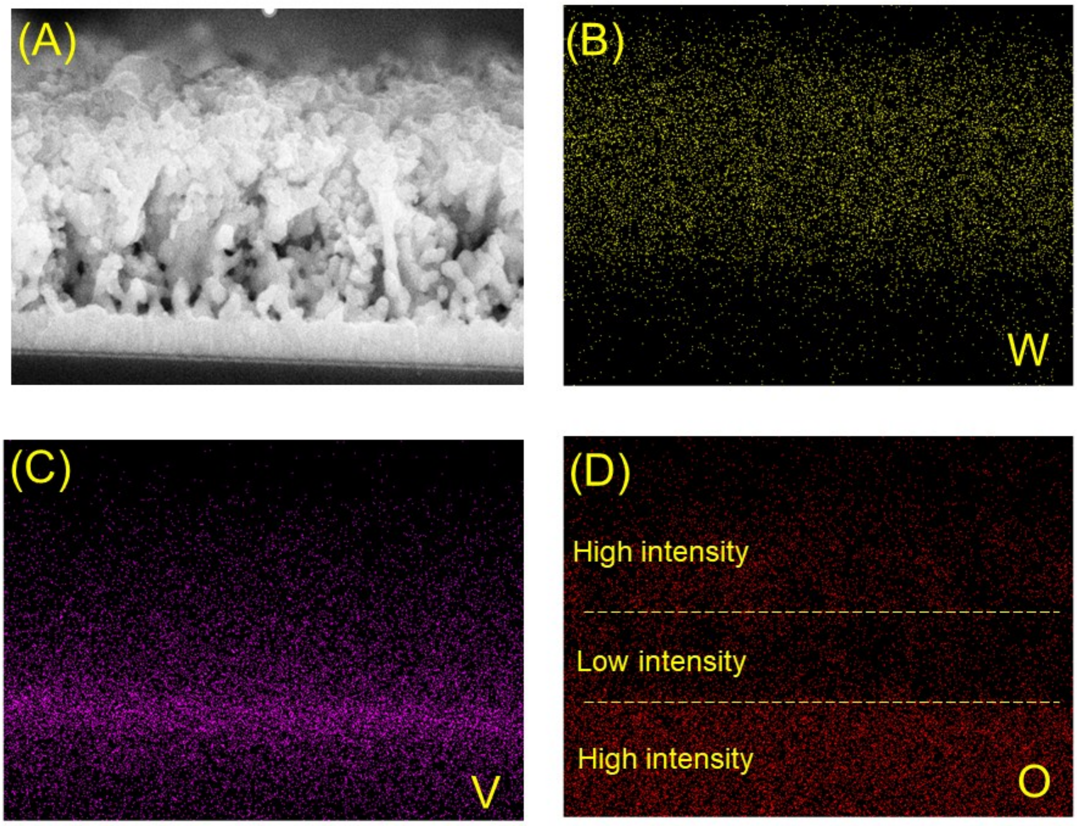

Figure S1. Cross-section EDS mapping of $BiVO_4$-W-WO_3-3200.

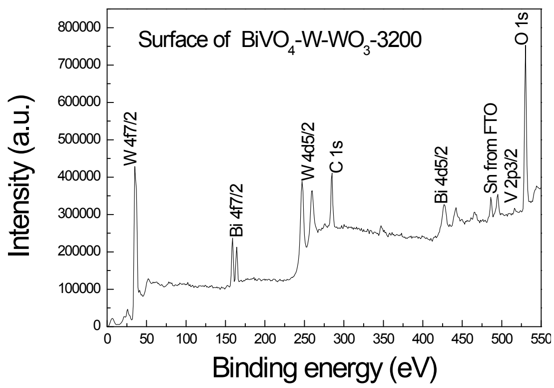

Figure S2. Survey surface-XPS result of the $BiVO_4$-W-WO_3-3200.

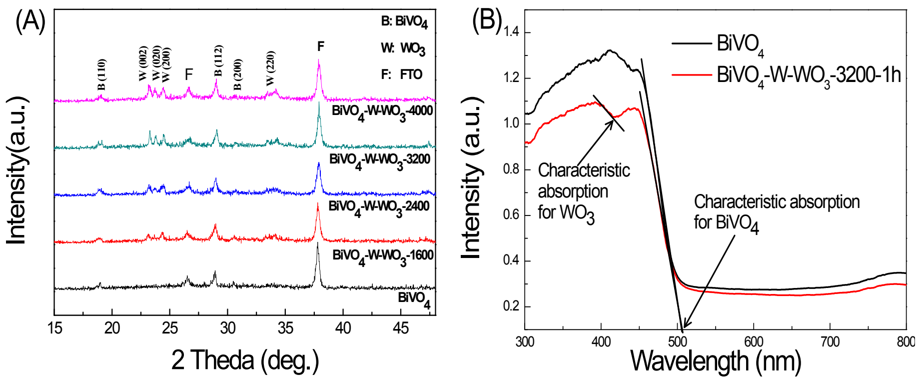

Figure S3. (A) XRD of $BiVO_4$ and $BiVO_4$-W-WO_3 composite thin film. (B) UV-Vis diffuse reflection spectroscopy results of $BiVO_4$ and $BiVO_4$-W-WO_3-3200-1h.

Table S1. AFM root mean squared roughness results of these photoanodes

Sample	Raw Mean	Mean	Z Range	Surface Area	Projected Surface Area	Surface Area Difference	Rq	Ra	Rmax	Skewness	Kurtsis
$BiVO_4$	1391 nm	1.70 nm	432 nm	17.0 um^2	12.8 μm^2	33.2 %	56.9 nm	44.3 nm	433 nm	0.292 nm	3.41 nm
$BiVO_4/W/WO_3$	138 nm	- 1.56 nm	316 nm	19.1 um^2	15.8 μm^2	20.5 %	47.6 nm	38.0 nm	311 nm	-0.0613 nm	2.91 nm

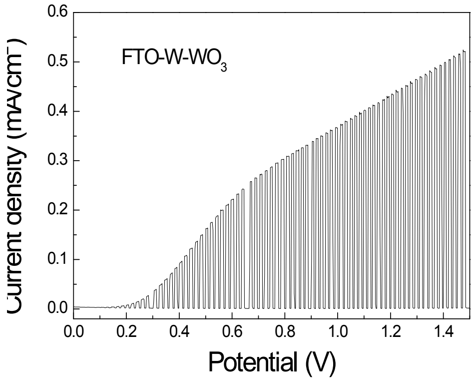

Figure S4. Photo-induced I-V curve of W-WO_3 photoanode on FTO substrate.

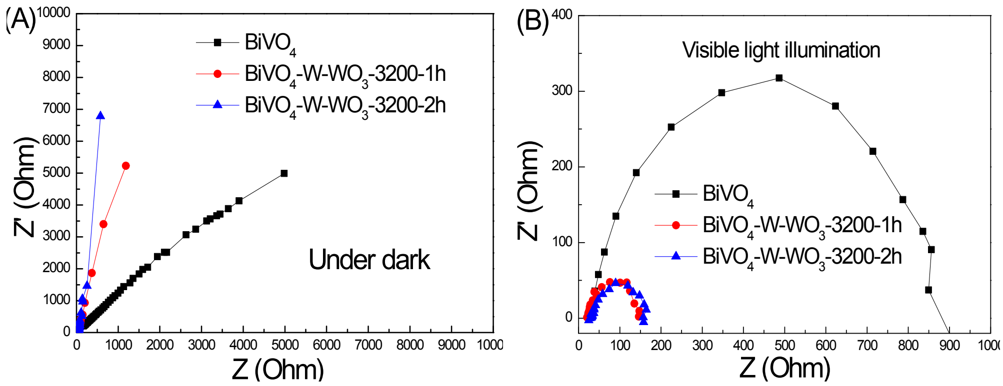

Figure S5. Electrochemical impedance spectroscopy (EIS) results of $BiVO_4$, $BiVO_4$-W-WO_3-3200- 1h, $BiVO_4$-W-WO_3-3200- 2h (A) under dark and (B) visible light illumination.

Table S2. Comparison of different $BiVO_4$ and WO_3 based photoanode systems used for solar water splitting

Photoanode material type	Onset potential	Current density at 1.23 V versus RHE	Light source	Electrolyte	References
Bilayer $WO_3/BiVO_4$ film	0.2 V	2.1 mA cm^{-2}	100 mW cm^{-2} Visible light	0.5 M Na_2SO_4 (pH = 7)	2
$WO_3/BiVO_4$ core/shell nanowire	0.6 V	3.1 mA cm^{-2}	100 mW cm^{-2} AM 1.5G	0.5 M potassium phosphate solution (pH = 8)	3
$WO_3/BiVO_4$ heterojunction	0.5 V	1.0 mA cm^{-2}	100 mW cm^{-2} AM 1.5G	0.5 M Na_2SO_4 (pH = 7)	4
Yolk-shell-shaped $WO_3/BiVO_4$ heterojunction	0.3 V	2.3 mA cm^{-2}	100 mW cm^{-2} AM 1.5G	0.5 M Na_2SO_4	5
3D $WO_3/BiVO_4$-Co-Pi	0.05 V	4.5 mA cm^{-2}	100 mW cm^{-2}	0.5 M Na_2SO_4	6

inverse opal			AM 1.5G	(pH = 6.8)	
1D $WO_3/BiVO_4$/Co-Pi Heterojunction	0.2 V	3.8 mA cm^{-2}	100 mW cm^{-2} AM 1.5G	0.1 M Na_2SO_4 (pH = 7)	7
$WO_3/BiVO_4$+Co-Pi core-shell nanostructure	- 0.5 V	6.72 mA cm^{-2}	100 mW cm^{-2} AM 1.5G	potassium phosphate solution (pH = 7)	8
WO_3-NRs/$BiVO_4$ modified with Co-Pi	0.5 V	3.2 mA cm^{-2}	100 mW cm^{-2} AM 1.5G	0.5 M Na_2SO_4	9
$WO_3/BiVO_4/TiO_2$ heterojunction	0.1 V	4.2 mA cm^{-2}	100 mW cm^{-2} AM 1.5G	0.1 M Na_2SO_4	10
$BiVO_4$/W/WO_3 Z-Scheme	0.05 V	4.5 mA cm^{-2}	100 mW cm^{-2} Visible light	0.1 M Na_2SO_4 (pH = 7)	This work

Reference

1 T. W. Kim, K.S. Choi, *Science*, 2014, **343**, 990.
2 M. G. Mali, H. Yoon, M. Kim, M.T. Swihart, S.S. Al-Deyab a, S.S. Yoon, *Appl. Phys. Lett.*, 2015, **106**, 151603.
3 P. M. Rao, L. Cai, C. Liu, I. S. Cho, C. H. Lee, J. M. Weisse, P. Yang, X. Zheng, *Nano Lett.*, 2014, **14**, 1099.
4 I. Grigioni, K.G. Stamplecoskie, E. Selli, P.V. Kamat, *J. Phys. Chem. C*, 2015, **119**, 20792.
5 B. Jin, E. Jung, M. Ma, S. Kim, K. Zhang, J.I. Kim, Y. Son, J.H. Park, *J. Mater. Chem. A*, 2018, **6**, 2585.
6 H. Zhang, W. Zhou, Y. Yang, C. Cheng, *small*, 2017, **13**, 1603840.
7 S. Y. Chae, H. Jung, H.S. Jeon, B.K. Min, Y.J. Hwang, O.S. Joo, *J. Mater. Chem. A*, 2014, **2**, 11408.
8 Y. Pihosh, I. Turkevych, K. Mawatari, J. Uemura, Y. Kazoe, S. Kosar, K. Makita, T. Sugaya, T. Matsui, D. Fujita, M. Tosa, M. Kondo, T. Kitamori, *Sci. Rep.*, 2015, **5**, 11141.
9 Y. Pihosh, I. Turkevych, K. Mawatari, T. Asai, T. Hisatomi, J. Uemura, M. Tosa, K. Shimamura, J. Kubota, K. Domen, T. Kitamori, *small*, 2014, **10,** 3692.
10 S. S. Kalanur, I. H. Yoo, J. Park, H. Seo, *J. Mater. Chem. A*, 2017, **5**, 1455.